

The combined effects of Map3k1 mutation and dioxin on differentiation of keratinocytes derived from mouse embryonic stem cells

Jingjing Wang

University of Cincinnati Medical Center

Bo Xiao

University of Cincinnati Medical Center

Eiki Kimura

University of Cincinnati Medical Center

Maureen Mongan

University of Cincinnati Medical Center

Ying Xia (✉ ying.xia@uc.edu)

University of Cincinnati Medical Center

Article

Keywords:

Posted Date: March 28th, 2022

DOI: <https://doi.org/10.21203/rs.3.rs-1451126/v1>

License:  This work is licensed under a Creative Commons Attribution 4.0 International License.

[Read Full License](#)

Abstract

Epithelial development starts with stem cell commitment to ectoderm followed by differentiation to basal keratinocytes. The basal keratinocytes, first committed in embryogenesis, constitute the basal layer of the epidermis. They have robust proliferation and differentiation potential, giving rise to suprabasal cells, and are responsible for expansion, maintenance and regeneration of the epidermis. We generated basal epithelial cells *in vitro* through differentiation of mouse embryonic stem cells (mESCs). Early on in differentiation, the expression of stem cell markers, *Oct4* and *Nanog*, decreased rapidly along with increased ectoderm marker *keratin (Krt) 18*. Later on, *Krt 18* expression was subdued when cells displayed basal keratinocyte characteristics, including regular polygonal shape, adherent and tight junctions and *Krt 14* expression. Using *Map3k1* mutant mESCs and environmental dioxin, we examined the gene and environment effects on differentiation. Neither *Map3k1* mutation nor dioxin altered mESC differentiation to ectoderm and basal keratinocytes, but they, individually and in combination, potentiated *Krt 1* expression and basal to spinous differentiation. Similar gene-environment effects were observed *in vivo* where dioxin exposure increased *Krt 1* more substantially in the epithelium of *Map3k1^{+/-}* than wild type embryos. Thus, the *in vitro* model of epithelial differentiation can detect genetic and environmental effects on epidermal development.

Introduction

The development of the epidermis is a consecutive multi-step process that commences at the differentiation of stem cell to surface ectoderm, which in turn differentiates to the keratinocytes (1, 2). Keratinocytes are the principal constituents of the epidermis, which is composed of four layers, basal, spinous, granular and cornified envelop. Cells in each layer have distinct morphological and biochemical properties and gene expression (3). The basal keratinocytes express keratins (*Krt*) 5 and *Krt 14*, the spinous keratinocytes express *Krt 1* and *Krt 10*, and the granular and cornified keratinocytes express Involucrin, Loricrin and Filaggrin (4). Only the basal keratinocytes are capable of proliferation, and they serve as the reservoir to supply and replenish cells in the suprabasal layers.

Disruption of the differentiation program of the epidermis leads to developmental defects (5–9). Skin abnormalities, such as neurofibromatosis, xeroderma pigmentosum, epidermolysis bullosa, and the most common psoriasis and atopic eczema, are costly congenital disorders that often require lifetime health care (10). Mutations of genes associated with epithelial differentiation account for some anomaly cases, whereas environmental factors acting through epigenetic modulations are also known to be an etiology for the diseases (11–14). Up to date, the genetic and environmental etiology for many skin disorders has remained poorly understood.

MAP3K1, also known as MEK Kinase 1 (MEKK1), is a member of the MAP3K superfamily, and plays highly specific roles in signal transduction and embryonic development (15). MAP3K1 deficient mice have a birth defect of the eye, due to abnormal epithelial morphogenesis in the embryonic eyelids (16, 17). While how MAP3K1 affects epithelial morphogenesis is still under investigation, the gene expression

signatures in epithelial cells isolated from wild type and *Map3k1* knockout mice show that MAP3K1 may impede basal to suprabasal differentiation (18). This role of MAP3K1, however, had neither been validated nor further explored.

The dioxin-like chemicals (DLCs) represent a large group of chemicals that are wide-spread environmental contaminants (19). The DLCs are generated either naturally through processes like forest fires and volcanic eruptions or by industrial activities, such as incomplete combustions. These chemicals are stable in the environment with a half-life of several years. Therefore, human exposure is inevitable. DLC exposure has been linked to many developmental defects (20–23). Using 2,3,7,8-Tetrachlorodibenzo-p-dioxin (TCDD) as a model DLC congener, studies in laboratory rodents show that *in utero* dioxin exposure causes diverse developmental abnormalities, including, but not limited to, hydronephrosis, cleft palate, and vaginal thread formation (24). In the epidermis, dioxin is shown to accelerate terminal differentiation, leading to acanthosis and epidermal hyperkeratosis phenotypes in mice and potentiate terminal differentiation of human keratinocytes *in vitro* (25, 26). Moreover, dioxin enhances differentiation of cells that have already committed to differentiation, insinuating that this environmental toxicant affects differentiation in a developmental stage-specific manner (27).

Mouse embryonic stem cells (mESCs) are the inner cell mass cells isolated from the pre-implantation blastocysts (28, 29). When maintained under a well-defined culture condition, the mESCs have unlimited capacity of self-renewal, remain pluripotent with abundant expression of the pluripotency genes, such as *Oct3/4 (Pou5f1)* and *Nanog* (30, 31). The mESCs also have potent potential of differentiation to generate all the cell types of the body (32). Under defined inducing conditions, they produce cells of the three primary germ layers, i.e. mesoderm, definitive endoderm and ectoderm, which in turn give rise to progenitor and mature cells of various lineages. Differentiation of mESC to generate epithelial cells for the purpose of tissue engineering and wound healing has been reported (33, 34), but it has not been used to explore the genetic and/or environmental factors as the underlying etiology of epithelial disorders.

In this study, we differentiated mESCs to basal keratinocytes *in vitro*. Retinoic acid (RA) and bone-morphogenetic protein-4 (BMP4) were used to induce early stage commitment of the surface ectodermal lineages; Defined keratinocyte serum free medium (DKSFM) were used to drive further differentiation to and the expansion of basal keratinocytes. The resultant basal keratinocytes could be passaged at least 20 times with minimal terminal differentiation. Using this system, we investigated the effects of the environmental toxicant dioxin and *Map3k1* gene mutations, either individually or in combination, on epidermal differentiation. The results highlight the utility of the *in vitro* system to investigate risk factors and multifactorial etiology in congenital skin disorders without extensive utilization of live animals.

Results

In vitro differentiation of mouse ESCs to keratinocyte. We differentiated the mESCs *in vitro* using a protocol adapted from Bilousova et. al. and Metallo et al. with modifications to increase efficiency at the initial phase of the procedure (35, 36) (Fig. 1A). Specifically, mESCs were re-suspended in EB media and

the hanging drop methods were used for EB formation. Under these conditions, compact, sphere-shaped EBs formed in nearly 80% of the hanging drops (Fig. 1B). After plating on CollV-coated plates and growing in DKSM media, the EBs had many cells growing out from the center (Fig. 1C). The outgrown cells displayed predominant ectodermal characteristics with strong expression of the surface ectodermal marker Krt 18. After passage and culture for 21–60 days, the cells started to exhibit basal keratinocyte-like morphology with increased expression of the basal keratinocyte marker Krt 14 (Figs. 1D and 1E). At approximately passage 6 (P6), the cells began to express abundant Krt 14 that was sustained subsequently in at least 20 passages. The cells can also be stored in and recovered from liquid N₂ with no apparent change of basal keratinocyte morphology and Krt 14 expression.

Examination of the cells at mRNA level at different days of *in vitro* culture revealed a gradual decrease of the expression of stem cell markers, *Oct4* and *Nanog*, which reached undetectable expression levels by day 9. Conversely, there was a significant increase in the expression of *Krt 18* (Figs. 2A and 2B). The *Krt 18* expression reached peak levels at 8–13 days of differentiation, but decreased sharply afterwards, and remained at a steady low level at the 4th passage and onward. Concurrently, the *Krt 14* expression increased gradually and arrived at a steady high level after a few passages (Fig. 2C). Cells in the later passages also exhibited a slight expression of suprabasal gene, *Krt 1*, but had no detectable *Fillagrin* (*Flg*) that is expressed only in the uppermost layer of the epidermis at late stage of fetal development (Fig. 2D). The adherence junctions and tight-junctions, key characteristics of the basal keratinocytes detected by E-cadherin and ZO-1 staining, were evidently formed at the intercellular contacts (Fig. 2E) (37, 38). These cells maintained a high level of Krt 14 expression for > 20 passages, including after recovery from storage in liquid N₂, and are henceforth termed differentiated-keratinocyte (D-KC).

The role of MAP3K1 in keratinocyte differentiation. MAP3K1 is a signal transduction enzyme playing key roles in embryonic development, specifically in epithelial morphogenesis (16). Although the *Map3k1*^{-/-} mice do not have overt skin defects, they display eye developmental defects due to abnormal epithelial morphogenesis and delayed healing of skin full-thickness wounds (18). To explore the role of MAP3K1 in skin biology, we re-analyzed the global gene expression in wild type and *Map3k1*^{-/-} primary keratinocytes (18), using a more stringent cut-off criteria and performed GO analyses of the differentially expressed genes. We found that skin development was a top biological process affected by MAP3K1 (Fig. 3A). Specifically, genes in epithelial terminal differentiation were significantly up-regulated in the *Map3k1*^{-/-} versus wild type cells (18) (S1 Table).

To evaluate whether the roles of MAP3K1 in epithelial differentiation could be recapitulated *in vitro*, wild type and *Map3k1*^{-/-} mESCs were used for *in vitro* differentiation and the expression of marker genes were examined at different time intervals. Wild type and *Map3k1*^{-/-} cells had similar expression of *Krt 18* at the early phase of differentiation (Fig. 3B). While these cells also had similar *Krt 14* expression, they were strikingly different on *Krt 1* expression at the later phase of differentiation (Fig. 3C). The expression levels of *Krt 1* were 10-fold more abundant in *Map3k1*^{-/-} than in wild type cells, suggesting that loss of MAP3K1 accelerated differentiation from basal to suprabasal keratinocytes. Thus, the *in vitro* system

validated the role of MAP3K1 in hampering epithelial terminal differentiation originally insinuated from global gene expression.

Dioxin potentiate keratinocyte differentiation *in vitro*. The global environmental pollutant dioxin exhibits diverse developmental toxicities and is suggested to cause acanthosis and epidermal hyperkeratosis through derailing epithelial differentiation (25). As most dioxin effects are mediated by the Aryl Hydrocarbon Receptor (AHR), a ligand-activated transcription factor that regulate dioxin-responsive genes (39), we examined AHR expression during *in vitro* epithelial differentiation. The expression of *Ahr* was negligible in mESCs, but was significantly increased as soon as the cells started to differentiate in the EBs at day 2 of differentiation, consistent with previous observations (40) (Fig. 4A). The *Ahr* expression continuously increased and remained at high levels after the cells committed to primary ectodermal lineages and became basal keratinocytes, suggesting that AHR signaling could be activated by dioxin as soon as the cells exit stemness.

To evaluate the effects of dioxin on differentiation, we examined cells differentiated in media with or without dioxin for 13 days. The presence of dioxin in the culture media did not alter the expression of *Krt 18* and *Krt 14*, suggesting that dioxin did not change the course of differentiation from mESC to surface ectoderm and basal keratinocytes (Fig. 4B). After multiple passages (> 8), the steady-state D-KC exhibited a robust dioxin-induced AHR activation, reflected by the induction of *Cyp1a1*, the prototypical AHR target gene (Fig. 4C). While the presence of dioxin did not change *Krt 14* expression, it increased *Krt 1* expression by 3-fold. Hence, dioxin potentiates basal to spinous keratinocyte differentiation.

Dioxin plus Map3k1 loss-of-function further promote differentiation. *In vivo*, dioxin and *Map3k1^{+/-}* have synergistic effects on impairing eye development. When neither dioxin nor *Map3k1^{+/-}* alone are detrimental, their combination causes birth defects of the eye, a defect observed also in un-treated *Map3k1^{-/-}* mice (41). Notwithstanding the intriguing phenotypic observations, how the environmental and genetic factors converge to disrupt the developmental programs has remained elusive. Given the similar effects of dioxin and *Map3k1* gene mutation on promoting suprabasal differentiation, we postulated that the combination of these conditions exacerbated the differentiation abnormalities. We tested the idea by treatment of D-KC derived from wild type and *Map3k1^{+/-}* mESCs with 10 nM dioxin for 3 days and examination of *Krt 1* expression. Compared to the wild type cells, the *Map3k1^{+/-}* cells had an increase of *Krt 1* expression (Fig. 5A). Dioxin treatment increased *Krt 1* expression by 3-fold in wild type cells, and remarkably, it induced *Krt1* expression further in *Map3k1^{+/-}* cells. The *Krt 1* expression in dioxin-treated *Map3k1^{+/-}* cells reached to nearly 8-fold of the levels in the untreated wild type cells and close to the levels in the untreated *Map3k1^{-/-}* cells (Figs. 3C and 5A).

We also tested this idea *in vivo* by treatment of pregnant mice, carrying wild type and *Map3k1^{+/-}* embryos, with 50 ug/kg dioxin on embryonic day (E)11.5. The embryos were collected on E15.5, as described previously (41) and the embryonic skin was examined by immunohistochemistry. The E-cadherin staining labeled multiple layers of the epithelial cells in the embryonic skin, in which the Krt 1

positive cells were detectable at the most outer layer (Fig. 5B). Quantification of the signal intensities showed that neither dioxin exposure nor *Map3k1*^{+/-} altered the level of Krt 1 expression; however, their combination significantly increased Krt 1 in more than 20 samples examined (Fig. 5C). The *in vivo* and *in vitro* data together raise an intriguing possibility that the gene-environment interactions significantly potentiate basal to suprabasal differentiation as a potential mechanism underlying the eye developmental abnormalities.

Discussion

In this paper, we describe an experimental system that differentiates mESCs to basal keratinocytes *in vitro*. The system enables convenient incorporation of genetic and environmental components, leading to the findings that *Map3k1* loss-of-function and dioxin, while do not affect mESC differentiation to surface ectoderm and basal keratinocytes, jointly potentiate basal to suprabasal epidermal differentiation. Compelled by these *in vitro* findings, we examined the gene-environment interactions *in vivo* and found that *in utero* dioxin exposure indeed increased Krt 1 expression more abundantly in the *Map3k1*^{+/-} than in the wild type embryos. These data suggest that the *in vitro* system described here can be used to explore complex conditions and etiology in the perturbation of epithelial differentiation.

Dioxin is a ubiquitous environmental agent that is stable and persistent in the environment and biological systems (42). Consistent with the notion that most toxic effects of dioxin are mediated through the AHR, we found a good correlation between *Ahr* expression and dioxin effects on differentiation (43). The minimal *Ahr* expression in mESCs and early phase of differentiation corresponded with unaltered differentiation from mESC to progenitor to basal keratinocytes in the presence of dioxin. The gradually increased *Ahr* and the steady-state high expression in the basal keratinocytes corresponded to potentiation of basal to spinous differentiation by dioxin. A similar observation has been made in the human cell culture models where dioxin is found to accelerate keratinocyte terminal differentiation, but does not change proliferation and apoptosis (26, 27). It is worth noting that of the many clinical manifestations of dioxin exposure, chloracne, a hyperkeratotic skin disorder is the most consistent pathology observed in exposed humans (44, 45). Thus, potentiation of basal to spinous differentiation observed in here is likely relevant to dioxin-induced skin pathogenesis.

How dioxin accelerates differentiation remains unclear. Dioxin treatment of basal keratinocytes led to a significant up-regulation of *Cyp1a1*, an AHR-regulated detoxification gene. However, the detoxification gene products have not been causally linked to *Krt 1* expression and differentiation. The dioxin-AHR axis also regulates expression of genes that are not implicated in detoxification, such as transforming growth factor- α , epidermal growth factor(46), Interleukin-1b and Plasminogen activator inhibitor-2 (47). Some of these gene products may mediate the toxicities of dioxin. For example, in a mouse model of embryonic palate fusion, Abbott et. al. showed that dioxin induces epithelial differentiation abnormalities to cause cleft palate in wild type, but not *Egf* knockout mouse palates, implicating a role for EGF in dioxin toxicity (48).

We have previously shown that MAP3K1 is a signaling molecule crucial for eye development and that the *Map3k1*^{-/-} but not *Map3k1*^{+/-} embryos have eyelid closure defects due to epithelial morphogenetic abnormalities (16). More recently, we found that *Map3k1* gene mutations sensitize the developmental programs to the toxicity of dioxin-like environmental chemicals (41). Specifically, *in utero* dioxin exposure induces eye defects in *Map3k1*^{+/-} but not wild type embryos. The *in vitro* mESC epithelial differentiation model suggests that the gene (*Map3k1*)-environment (dioxin) interactions affect epithelial differentiation, followed by *in vivo* validation. The *in vitro* and *in vivo* data present a coherent narrative that *Map3k1* mutation and dioxin promote basal to suprabasal differentiation, which is further potentiated by both agents together. The differentiation abnormalities induced by dioxin plus *Map3k1*^{+/-} resemble those in *Map3k1*^{-/-} cells, raising an intriguing possibility that the developmental defects occur when the differentiation abnormalities reaching beyond a threshold level.

Our differentiation protocol is modified from Metallo et. al. and Bilousova, et. al. with improved efficiency (35, 36, 49). Using this protocol, we detected a gradual increase of *Krt 18* expression, reaching the peak level in 10 days that are comparable to the time frame required for mouse stem cells to commit to ectodermal lineage *in vivo* (50). We further obtained Krt 14-expressing cells after culturing for approximately a month, though this time frame was much longer than that took *in vivo* for ectodermal to basal epithelial cell conversion. Given that the Krt 18-positive to Krt 14-positive conversion requires DNA methylation to turn off the *Krt 18* promoter and multiple extracellular signals and transcription factors to activate the *Krt 14* promoter, we speculate that these epigenetic and transcription machineries are less robust *in vitro* than *in vivo* (51–53).

In vivo, the basal layer epidermis has low Ca²⁺ concentrations that support basal keratinocyte proliferation, whereas the suprabasal layers have high Ca²⁺ concentrations to promote terminal differentiation. Additionally, the three-dimensional (3D) *in vivo* microenvironment facilitate the intricate cell-matrix interactions and differentiation gene expression (54). The *in vitro* conditions, i.e. monolayer culture and the DKFSM media containing 0.15 mM calcium similar to the Ca levels in the basal layer epidermis, on the other hand, seem to favor basal keratinocyte proliferation but prevent differentiation (55, 56). Therefore, the Krt 14-positive cells can be extensively sub-cultured with stable basal keratinocyte characteristics.

In summary, we have established an experimental model that differentiates mESCs to keratinocytes that recapitulates epithelial differentiation from E3.5 to E15.5. This system can be used as a convenient tool to trace epithelial differentiation; the resultant basal keratinocytes can be amplified and cultured for a long period of time, serving as resources for epithelial molecular biology research. Using this system, we show that *Map3k1* loss-of-function mutation and dioxin act jointly to potentiate epithelial spinous differentiation, unveiling a potential mechanism through which gene-environment interactions, but not each agent separately, cause developmental abnormalities. Understanding the complex etiology of diseases will help the development of preventive strategies.

Materials And Methods

Reagents, antibodies and chemicals. Soybean Trypsin Inhibitor (17075-029), TrypLE and Defined Keratinocyte SFM (DKSFM) were from Gibco. Dulbecco's Modification of Eagle's Medium (DMEM; 10-017-CV) was purchased from Corning. Collagen (Col) IV (354233) was from BD Biosciences. ESGRO Leukemia Inhibitory Factor (LIF) (10^7 U/ml, ESG1107), retinoic acid (RA; 302-79-4) and Hoechst 33342 (B2261) were from Sigma; recombinant mouse bone morphogenetic protein-4 (BMP4; 120-05ET) was from PEPROTECH. Dioxin, i.e. TCDD, was from AccuStandard and dissolved in dimethyl sulfoxide (DMSO; 67-68-5, Sigma). The rest cell culture media and reagents, and antibodies are listed in S2 and S3 Tables.

Mice, mESC culture and differentiation. The wild type and *Map3k1*^{+/-} mice, *in utero* dioxin exposure and the collection and process of embryos for immunostaining were described before (41). The wild type, *Map3k1*^{+/-} and *Map3k1*^{-/-} mESCs were obtained from pregnant mice as described (57). The mESCs were expanded and maintained in DMEM supplemented with 15% Knockout™ Serum Replacement (Gibco), LIF (10000x), 2 mM glutamine, 1% nonessential amino acids, 1 mM sodium pyruvate, 2-mercaptoethanol (Gibco, 1000x), 100 U/ml penicillin and 100 µg/ml streptomycin (Cytiva), in a humidified incubator with 5% CO₂ at 37°C. Protocol describing mouse experiments and procedures was approved by IACUC of the University of Cincinnati, and all experiments were performed in accordance with UC guidelines and regulations.

The step-wise differentiation of mESCs to the epithelial lineages followed protocols in Bilousova, et. al. (35) and Metallo, et. al. (36) with modifications. Briefly, on day 0, mESCs were trypsinized and resuspended in DMEM with 15% fetal bovine serum (FBS), known as embryoid body (EB) media; cells (5×10^4 cells/25 µl) were placed as droplets on a Petri dish lid and incubated as “hanging drops” to enable the formation of EBs that contained cells of the three primitive germ layers (32). On day 2, the EBs (about 100 in number) were collected and transferred to a 100 mm ColIV-coated tissue culture dish in EB medium plus 1 µM RA and 25 ng/ml BMP4, conditions that selectively induce surface ectoderm differentiation. On day 4, media were changed to DKSFM plus RA and BMP4 to promote epithelial lineage differentiation. On day 8, media were changed to DKSFM for keratinocyte amplification. On day 13, many cells with epithelial morphology were moving outward from the EB center. The clumps at the EB center was removed by vacuum aspiration; the remaining cells were detached with TrypLE, resuspended in DKSFM containing 10 mg/ml trypsin inhibitor and passaged to a new ColIV-coated dish, as passage (P)1. The passaged cells can be continuously passaged for at least 20 generations and storage in and recover from liquid N₂. In some experiments, dioxin (10 nM) were included in the media at different phases of culture.

RNA isolation, reverse transcription and quantitative polymerase chain reaction (qPCR). Total RNA was isolated using PureLink RNA Mini Kit (12183025) and reverse transcription was performed using SuperScript IV reverse transcriptase (18090010; Invitrogen) following manufacture's protocols. qPCR was carried out using PowerUp SYBR Green Master Mix (4367659, Applied Biosystems) and the signals were detected with an Agilent Technologies Stratagene Mx3000P PCR machine. The PCR reactions ran for 40

cycles under the appropriate parameters for each pair of primers and fluorescence values were used to construct the amplification curve. Specifically, at 95°C for 10s and 60°C for 1 min. A dissociation curve was performed after amplification by gradual rise in temperature from 65 to 95°C with fluorescence signal measurement every 0.5°C. The results were normalized using *Gapdh*; $\Delta\Delta Ct$ were used to calculate fold change. Data represent results of triplicates of 2 or more experiments. The sequences of PCR primers are listed in S4 Table.

Immunofluorescence, microscopic image and quantification. The embryonic tissue sections were processed and immunohistochemistry was done as described previously (16, 58). Briefly, the embryonic/fetal heads were fixed in 4% paraformaldehyde at 4°C overnight. The tissues were embedded in Optimal Cutting Temperature compound and frozen. The entire eye was processed for coronal sections at 12 μ M. Cells grown on CollIV-coated coverslips were fixed with 4% paraformaldehyde at 4°C for 10 min, permeabilized with PBS plus 0.2% Triton, and subjected to immunofluorescent staining. Primary antibodies were diluted at 1:100 and secondary antibodies and nucleus staining reagents were diluted at 1:400. Immunofluorescence and bright field images were captured using a Zeiss Axio microscope. For immunostaining of the embryonic tissues, the images were analyzed using the ImageJ software (National Institutes of Health, Bethesda, MD, USA). The epithelial cell layers expressing distinctive E-cadherin were outlined and the mean intensity values of Krt1 staining were measured. Krt1 level in the images was determined after background subtraction.

Global gene expression and pathway analyses. The wild-type and *Map3k1*^{-/-} primary mouse keratinocytes were subjected to high-density microarray hybridization; the differential gene expression was analyzed as reported before (18). Data are currently available in supplemental file of the paper (<https://www.ncbi.nlm.nih.gov/pmc/articles/PMC1525243>) while GEO submission is in process. The data were re-analyzed through identifying the significantly differential expressed genes using the cut-off criteria: log₂ fold change > 1 or < -1, False Discovery Rates (FDR) < 0.1, and intensity > 200, and the biological process enrichment using Metascape as previously described (59). The datasets generated and/or analyzed during the current study are available

Statistical Analyses. Means and standard deviations were calculated based on at least three independent experiments, and analyzed using student's two-tailed *t*-test. **p*, #*p* < 0.05, ***p* < 0.01 and ****p*, ###*p* < 0.001 were considered statistically significant.

Declarations

Acknowledgements

We thank Dr. Alvaro Puga for critical reading of the manuscript. Research presented in this paper is supported in part by NIH grants R01 EY15227, R01 HD098106 and P30ES006096.

Author contributions

JW, develop differentiation protocol, design experiments, data analyses and write manuscript; BX, perform experiments, data analyses and write manuscript; EK, data analyses; MM, provide research materials; YX, design experiments, data analyses, write manuscript.

Data availability statement

The datasets and cells generated during and/or analyzed during the current study are available from the corresponding author on reasonable request.

Additional Information

Competing Interests Statement

The author(s) declare no competing interests.

References

1. C. Byrne, M. Tainsky, E. Fuchs, Programming gene expression in developing epidermis. *Development* **120**, 2369–2383 (1994).
2. J. Pispa, I. Thesleff, Mechanisms of ectodermal organogenesis. *Dev Biol* **262**, 195–205 (2003).
3. R. L. Eckert, J. F. Crish, N. A. Robinson, The epidermal keratinocyte as a model for the study of gene regulation and cell differentiation. *Physiol Rev* **77**, 397–424 (1997).
4. S. M. Morley *et al.*, Temperature sensitivity of the keratin cytoskeleton and delayed spreading of keratinocyte lines derived from EBS patients. *J Cell Sci* **108 (Pt 11)**, 3463–3471 (1995).
5. G. B. Mann *et al.*, Mice with a null mutation of the TGF alpha gene have abnormal skin architecture, wavy hair, and curly whiskers and often develop corneal inflammation. *Cell* **73**, 249–261 (1993).
6. J. M. Carroll, M. R. Romero, F. M. Watt, Suprabasal integrin expression in the epidermis of transgenic mice results in developmental defects and a phenotype resembling psoriasis. *Cell* **83**, 957–968 (1995).
7. B. P. Korge, T. Krieg, The molecular basis for inherited bullous diseases. *J Mol Med (Berl)* **74**, 59–70 (1996).
8. C. Li, H. Guo, X. Xu, W. Weinberg, C. X. Deng, Fibroblast growth factor receptor 2 (Fgfr2) plays an important role in eyelid and skin formation and patterning. *Dev. Dyn* **222**, 471–483 (2001).
9. M. Chidgey *et al.*, Mice lacking desmocollin 1 show epidermal fragility accompanied by barrier defects and abnormal differentiation. *J. Cell Biol* **155**, 821–832 (2001).
10. D. M. Carter, A. D. Auerbach, L. J. Elsas, L. A. Goldsmith, A. W. Lucky, Dermatologic birth defects and congenital skin disease. *J Am Acad Dermatol* **11**, 974–983 (1984).
11. J. C. Chamcheu *et al.*, Keratin gene mutations in disorders of human skin and its appendages. *Arch Biochem Biophys* **508**, 123–137 (2011).

12. J. Fischer, E. Bourrat, Genetics of Inherited Ichthyoses and Related Diseases. *Acta Derm Venereol* **100**, adv00096 (2020).
13. E. Soares, H. Zhou, Master regulatory role of p63 in epidermal development and disease. *Cell Mol Life Sci* **75**, 1179–1190 (2018).
14. C. N. Perdigoto, V. J. Valdes, E. S. Bardot, E. Ezhkova, Epigenetic regulation of epidermal differentiation. *Cold Spring Harb Perspect Med* **4**, (2014).
15. Y. Xia *et al.*, MEK kinase 1 is critically required for c-Jun N-terminal kinase activation by proinflammatory stimuli and growth factor-induced cell migration. *Proc Natl Acad Sci U S A* **97**, 5243–5248 (2000).
16. L. Zhang *et al.*, A role for MEK kinase 1 in TGF-beta/activin-induced epithelium movement and embryonic eyelid closure. *Embo J* **22**, 4443–4454 (2003).
17. T. Yujiri, S. Sather, G. R. Fanger, G. L. Johnson, Role of MEKK1 in cell survival and activation of JNK and ERK pathways defined by targeted gene disruption. *Science* **282**, 1911–1914 (1998).
18. M. Deng *et al.*, A role for the mitogen-activated protein kinase kinase kinase 1 in epithelial wound healing. *Mol. Biol. Cell* **17**, 3446–3455 (2006).
19. L. S. Birnbaum, Developmental effects of dioxins and related endocrine disrupting chemicals. *Toxicol. Lett* **82–83**, 743–750 (1995).
20. M. W. Preslan, G. R. Beauchamp, Z. N. Zakov, Congenital glaucoma and retinal dysplasia. *J. Pediatr. Ophthalmol. Strabismus* **22**, 166–170 (1985).
21. B. Eskenazi, G. Kimmel, Workshop on perinatal exposure to dioxin-like compounds. II. Reproductive effects. *Environ Health Perspect* **103 Suppl 2**, 143–145 (1995).
22. L. Gaspari *et al.*, Prenatal environmental risk factors for genital malformations in a population of 1442 French male newborns: a nested case-control study. *Hum Reprod* **26**, 3155–3162 (2011).
23. R. Kishi *et al.*, Ten years of progress in the Hokkaido birth cohort study on environment and children's health: cohort profile–updated 2013. *Environ Health Prev Med* **18**, 429–450 (2013).
24. L. S. Birnbaum, The mechanism of dioxin toxicity: relationship to risk assessment. *Environ Health Perspect* **102 Suppl 9**, 157–167 (1994).
25. C. S. Muenyi *et al.*, Effects of in utero exposure of C57BL/6J mice to 2,3,7,8-tetrachlorodibenzo-p-dioxin on epidermal permeability barrier development and function. *Environ Health Perspect* **122**, 1052–1058 (2014).
26. J. A. Loertscher, C. A. Sattler, B. L. Allen-Hoffmann, 2,3,7,8-Tetrachlorodibenzo-p-dioxin alters the differentiation pattern of human keratinocytes in organotypic culture. *Toxicol Appl Pharmacol* **175**, 121–129 (2001).
27. K. W. Gaido, S. C. Maness, Regulation of gene expression and acceleration of differentiation in human keratinocytes by 2,3,7,8-tetrachlorodibenzo-p-dioxin. *Toxicol Appl Pharmacol* **127**, 199–208 (1994).

28. M. J. Evans, M. H. Kaufman, Establishment in culture of pluripotential cells from mouse embryos. *Nature* **292**, 154–156 (1981).
29. G. R. Martin, Isolation of a pluripotent cell line from early mouse embryos cultured in medium conditioned by teratocarcinoma stem cells, *Proc. Natl. Acad. Sci. U. S. A* **78**, 7634–7638 (1981).
30. F. A. Brook, R. L. Gardner, The origin and efficient derivation of embryonic stem cells in the mouse. *Proc Natl Acad Sci U S A* **94**, 5709–5712 (1997).
31. S. Ohtsuka, Y. Nakai-Futatsugi, H. Niwa, LIF signal in mouse embryonic stem cells. *JAKSTAT* **4**, e1086520 (2015).
32. G. Keller, Embryonic stem cell differentiation: emergence of a new era in biology and medicine. *Genes Dev* **19**, 1129–1155 (2005).
33. F. Ning *et al.*, Differentiation of mouse embryonic stem cells into dental epithelial-like cells induced by ameloblasts serum-free conditioned medium. *Biochem Biophys Res Commun* **394**, 342–347 (2010).
34. E. T. Uluer, H. S. Vatansever, H. Aydede, M. K. Ozbilgin, Keratinocytes derived from embryonic stem cells induce wound healing in mice. *Biotech Histochem* **94**, 189–198 (2019).
35. G. Bilousova, J. Chen, D. R. Roop, Differentiation of mouse induced pluripotent stem cells into a multipotent keratinocyte lineage. *J. Invest Dermatol* **131**, 857–864 (2011).
36. C. M. Metallo, L. Ji, J. J. de Pablo, S. P. Palecek, Retinoic acid and bone morphogenetic protein signaling synergize to efficiently direct epithelial differentiation of human embryonic stem cells. *Stem Cells* **26**, 372–380 (2008).
37. K. Pummi *et al.*, Epidermal tight junctions: ZO-1 and occludin are expressed in mature, developing, and affected skin and in vitro differentiating keratinocytes. *J Invest Dermatol* **117**, 1050–1058 (2001).
38. N. Kirschner, C. Bohner, S. Rachow, J. M. Brandner, Tight junctions: is there a role in dermatology? *Arch Dermatol Res* **302**, 483–493 (2010).
39. D. W. Nebert, A. Puga, V. Vasiliou, Role of the Ah receptor and the dioxin-inducible [Ah] gene battery in toxicity, cancer, and signal transduction. *Ann N Y Acad Sci* **685**, 624–640 (1993).
40. Q. Wang *et al.*, Ah Receptor Activation by Dioxin Disrupts Activin, BMP, and WNT Signals During the Early Differentiation of Mouse Embryonic Stem Cells and Inhibits Cardiomyocyte Functions. *Toxicol Sci* **149**, 346–357 (2016).
41. M. Mongan *et al.*, Gene-Environment Interactions Target Mitogen-activated Protein 3 Kinase 1 (MAP3K1) Signaling in Eyelid Morphogenesis. *J. Biol. Chem* **290**, 19770–19779 (2015).
42. B. M. Van den *et al.*, The 2005 World Health Organization reevaluation of human and Mammalian toxic equivalency factors for dioxins and dioxin-like compounds. *Toxicol. Sci* **93**, 223–241 (2006).
43. O. Hankinson, The aryl hydrocarbon receptor complex. *Annu Rev Pharmacol Toxicol* **35**, 307–340 (1995).

44. M. Moses, P. G. Prioleau, Cutaneous histologic findings in chemical workers with and without chloracne with past exposure to 2,3,7,8-tetrachlorodibenzo-p-dioxin. *J Am Acad Dermatol* **12**, 497–506 (1985).
45. P. A. Bertazzi, I. Bernucci, G. Brambilla, D. Consonni, A. C. Pesatori, The Seveso studies on early and long-term effects of dioxin exposure: a review. *Environ Health Perspect* **106 Suppl 2**, 625–633 (1998).
46. E. J. Choi, D. G. Toscano, J. A. Ryan, N. Riedel, W. A. Toscano, Jr., Dioxin induces transforming growth factor-alpha in human keratinocytes. *J Biol Chem* **266**, 9591–9597 (1991).
47. T. R. Sutter, K. Guzman, K. M. Dold, W. F. Greenlee, Targets for dioxin: genes for plasminogen activator inhibitor-2 and interleukin-1 beta. *Science* **254**, 415–418 (1991).
48. B. D. Abbott, L. S. Birnbaum, Effects of TCDD on embryonic ureteric epithelial EGF receptor expression and cell proliferation. *Teratology* **41**, 71–84 (1990).
49. C. M. Metallo, L. Ji, J. J. de Pablo, S. P. Palecek, Directed differentiation of human embryonic stem cells to epidermal progenitors. *Methods Mol. Biol* **585**, 83–92 (2010).
50. S. Liu, H. Zhang, E. Duan, Epidermal development in mammals: key regulators, signals from beneath, and stem cells. *Int J Mol Sci* **14**, 10869–10895 (2013).
51. A. Rossi, S. I. Jang, R. Ceci, P. M. Steinert, N. G. Markova, Effect of AP1 transcription factors on the regulation of transcription in normal human epidermal keratinocytes. *J Invest Dermatol* **110**, 34–40 (1998).
52. M. Tomic-Canic, D. Day, H. H. Samuels, I. M. Freedberg, M. Blumenberg, Novel regulation of keratin gene expression by thyroid hormone and retinoid receptors. *J Biol Chem* **271**, 1416–1423 (1996).
53. W. Y. Yu, J. M. Slack, D. Tosh, Conversion of columnar to stratified squamous epithelium in the developing mouse oesophagus. *Dev Biol* **284**, 157–170 (2005).
54. F. Pampaloni, E. G. Reynaud, E. H. Stelzer, The third dimension bridges the gap between cell culture and live tissue. *Nat Rev Mol Cell Biol* **8**, 839–845 (2007).
55. J. Wang, M. Mongan, X. Zhang, Y. Xia, Isolation and long-term expansion of murine epidermal stem-like cells. *PLoS One* **16**, e0254731 (2021).
56. H. Hennings *et al.*, Calcium regulation of growth and differentiation of mouse epidermal cells in culture. *Cell* **19**, 245–254 (1980).
57. V. Bryja, S. Bonilla, E. Arenas, Derivation of mouse embryonic stem cells. *Nat Protoc* **1**, 2082–2087 (2006).
58. A. Takatori *et al.*, Differential transmission of MEKK1 morphogenetic signals by JNK1 and JNK2. *Development* **135**, 23–32 (2008).
59. Y. Zhou *et al.*, Metascape provides a biologist-oriented resource for the analysis of systems-level datasets. *Nat Commun* **10**, 1523 (2019).

Figures

Figure 1

Differentiation of mESCs to keratinocytes *in vitro*. (A) Scheme of *in vitro* mESC to keratinocyte differentiation. Representative brightfield and immunofluorescent staining images of (B) cell aggregates and EBs on Day 2 (D2), (C) attached EBs grown in presence of RA and BMP4 for 6 days (D8) with cells outgrown from the EBs expressing Krt 18 and few cells at the most outer layer started to express Krt 14, (D) Passaged cells at day 21 of differentiation formed colonies with more Krt 14 positive cells, and (E) Majority cells became Krt 14 positive after multiple passages and culture for 1-2 months (D60). Scale bar represents 200 μ m.

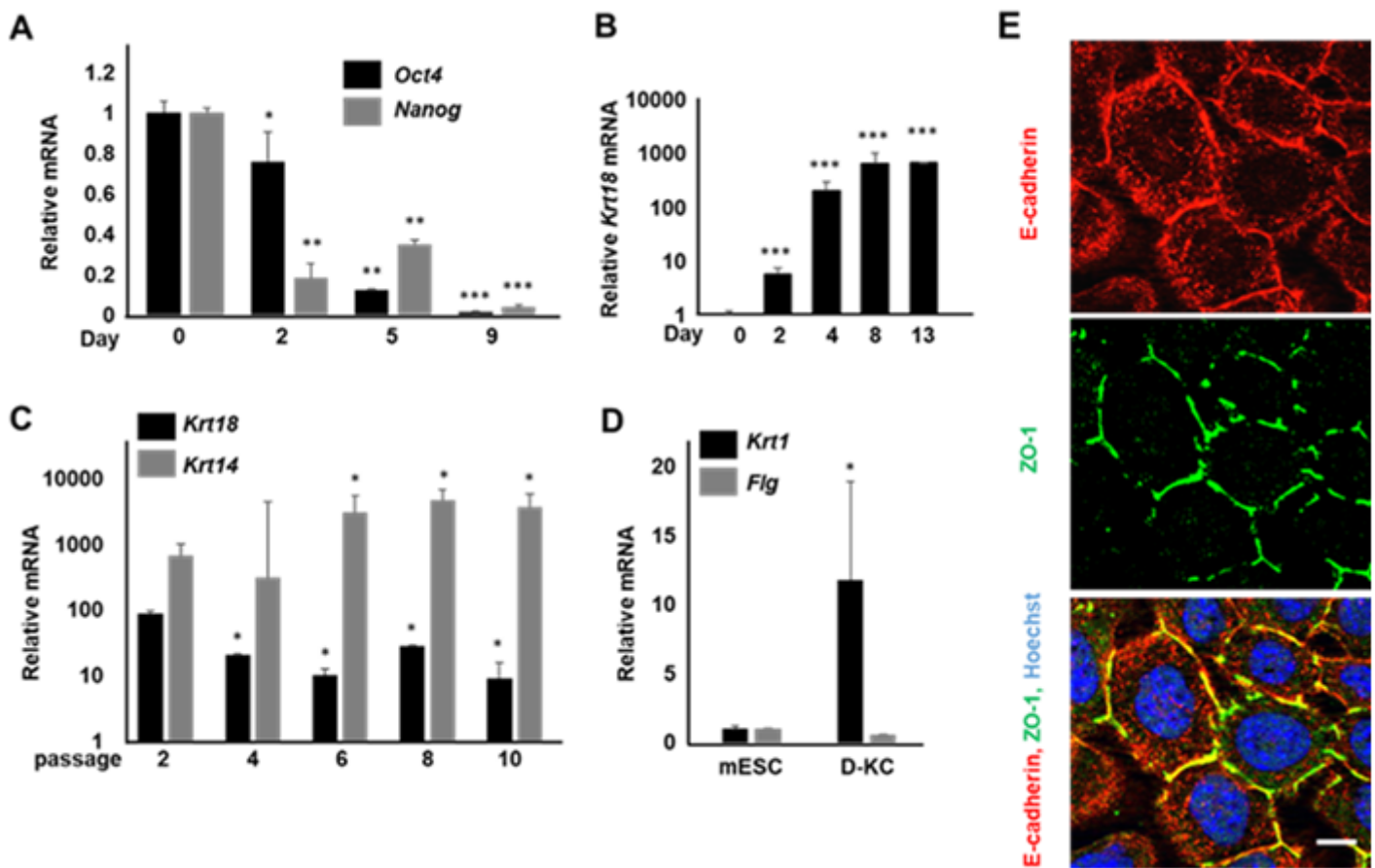


Figure 2

Molecular tracing of the *in vitro* differentiated cells. (A and B) Cells at different days of differentiation were examined for gene expression by RT-PCR. The expression of (A) the stem cell markers *Oct4* and *Nanog*, and (B) the ectoderm marker *Krt 18* were compared to the levels in undifferentiated mESCs, i.e. day 0. (C) Cells at different passages were examined for mRNA of *Krt 18* and *Krt 14*. The expression of *Krt 18* was significantly decreased while the expression of the basal keratinocyte marker *Krt 14* was

significantly increased with the increase of passages. High level *Krt 14* expression was stabilized at passage 6 onward. These cells are so forth termed differentiated-keratinocyte (D-KC). (D) Compared to mESCs, the D-KC had elevated expression of the spinous and granular cell marker *Krt 1*, but not the terminal differentiation and cornified envelop marker *Flg*. (E) D-KC were subjected to immunofluorescence staining for the adherence junction (E-cadherin) and tight junction (ZO-1), nucleus was stained with Hoechst 33342 (blue). * $p < 0.05$, ** $p < 0.01$, *** $p < 0.001$ were considered statistically significant compared to day 0 or passage 2. Scale bar represents 20 μm .

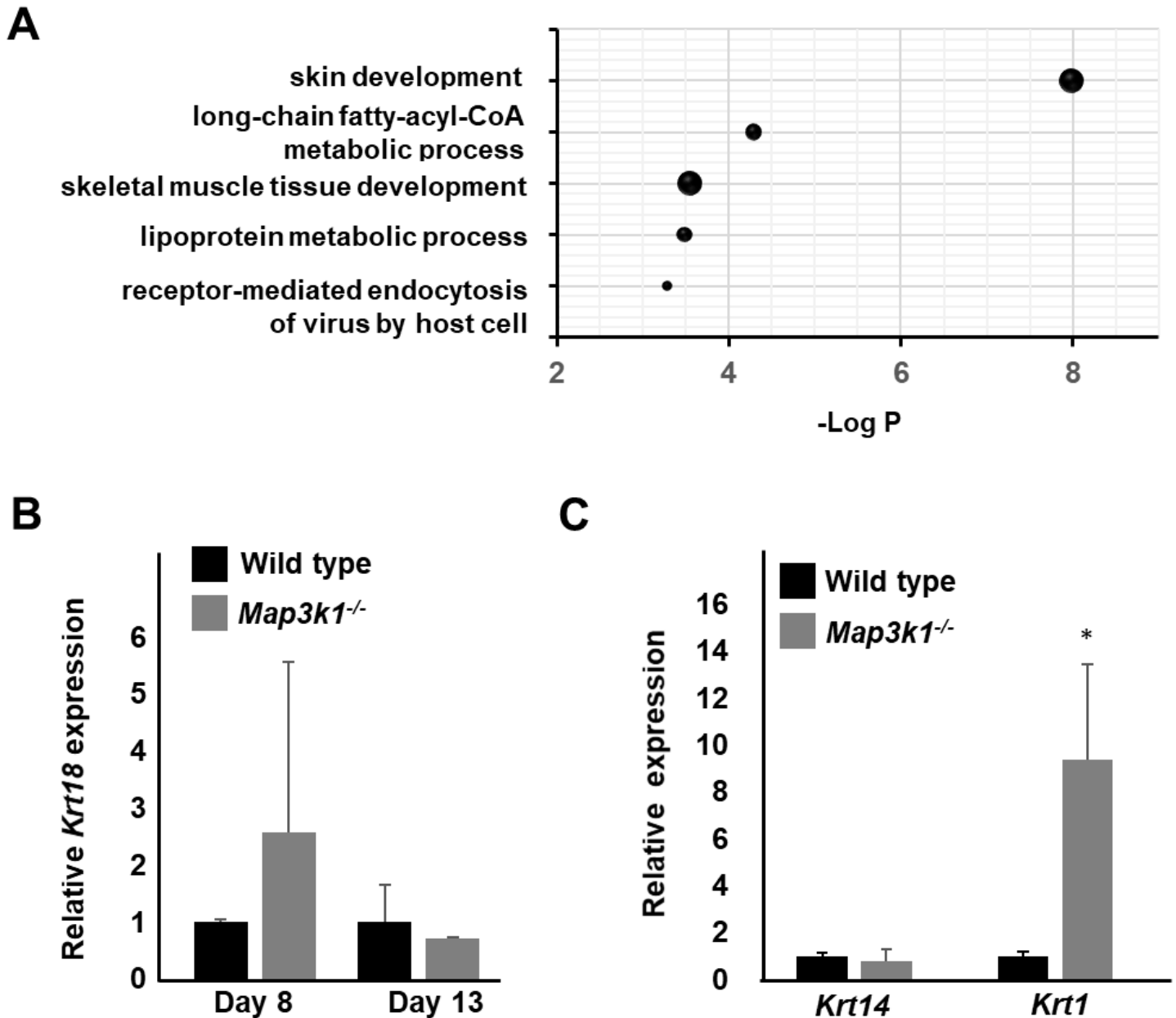


Figure 3

MAP3K1 loss-of-function enhanced suprabasal differentiation. (A) Differentially expressed genes in primary keratinocytes isolated from wild type and *Map3k1*^{-/-} mice were subjected to GO pathway analyses and the top biological functions up-regulated in the *Map3k1*^{-/-} versus wild type cells were shown. The wild type and *Map3k1*^{-/-} mESCs were differentiated *in vitro* for various times and examined for mRNA of (B) *Krt 18* at the early phases, and (C) *Krt 14* and *Krt 1* at the late phases (after 6 passages). The gene expression in *Map3k1*^{-/-} were compared to those in wild type cells, set as 1. *p<0.05 is considered statistically significant.

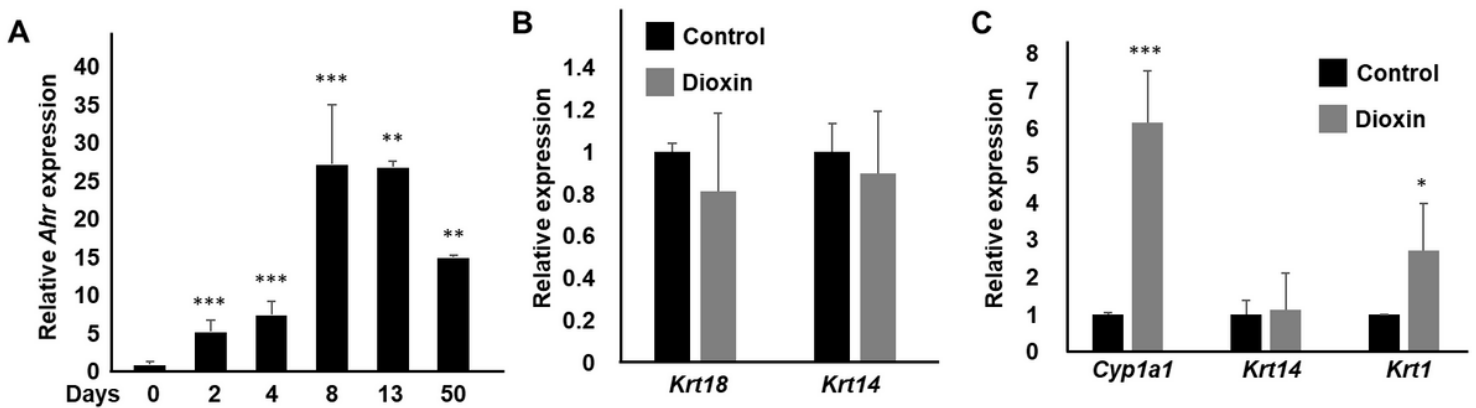


Figure 4

Dioxin potentiated suprabasal differentiation. Gene expression was examined using RT-PCR. (A) The *Ahr* expression was compared to levels in undifferentiated mESCs, set as 1. The expression of *Krt 18*, *Krt 14*, *Krt 1* and the AHR activation marker, *Cyp1a1* were examined (B) in cells differentiated for 13 days and (C) in D-KC, in the presence and absence of 10 nM dioxin. Statistical analyses and relative expression are based on comparison to (A) undifferentiated mESCs and (B) control samples, set as 1. *p<0.05, **p<0.01 and ***p<0.001 are considered significant.

Figure 5

Dioxin plus *Map3k1* loss-of-function potentiated keratinocyte terminal differentiation. The *Krt 1* expression was examined (A) by RT-PCR in wild type and *Map3k1*^{+/-} D-KC with or without 10 nM dioxin treatment for 3 days, and (B) by immunohistochemistry in wild type and *Map3k1*^{+/-} E15.5 embryos with or without 50 ug/kg dioxin treatment at E11.5; E-cadherin labeled all epithelial cells. (C) Quantification of Krt 1-positive signals. **p<0.01 are considered significantly different compared to wild type untreated

samples, and # $p < 0.05$, ### $p < 0.001$ are considered significantly different compared to untreated samples of the same genotype. Scale bar represents 50 μm .

Supplementary Files

This is a list of supplementary files associated with this preprint. Click to download.

- [supplementalinformation.docx](#)